ISSCR

Long-Term In Vitro Expansion of Salivary Gland Stem Cells Driven by Wnt Signals

Martti Maimets,[1,2] Cecilia Rocchi,[1,2] Reinier Bron,[1,2] Sarah Pringle,[1,2] Jeroen Kuipers,[1] Ben N.G. Giepmans,[1] Robert G.J. Vries,[4] Hans Clevers,[4] Gerald de Haan,[3] Ronald van Os,[3] and Robert P. Coppes[1,2,*]

[1]Department of Cell Biology, University Medical Center Groningen, University of Groningen, Antonius Deusinglaan 1, 9713 AV Groningen, the Netherlands
[2]Department of Radiation Oncology, University Medical Center Groningen, University of Groningen, PO Box 30001, 9700 RB Groningen, the Netherlands
[3]Department of Biology of Aging, Section Stem Cell Biology, European Research Institute for the Biology of Aging (ERIBA), University Medical Center Groningen, University of Groningen, Antonius Deusinglaan 1, 9713 AV Groningen, the Netherlands
[4]Hubrecht Institute, Royal Netherlands Academy of Arts and Sciences and University Medical Center Utrecht, 3584 CT Utrecht, the Netherlands
*Correspondence: r.p.coppes@umcg.nl
http://dx.doi.org/10.1016/j.stemcr.2015.11.009

SUMMARY

Adult stem cells are the ultimate source for replenishment of salivary gland (SG) tissue. Self-renewal ability of stem cells is dependent on extrinsic niche signals that have not been unraveled for the SG. The ductal compartment in SG has been identified as the location harboring stem cells. Here, we report that rare SG ductal EpCAM^{+} cells express nuclear β-catenin, indicating active Wnt signaling. In cell culture experiments, EpCAM^{high} cells respond potently to Wnt signals stimulating self-renewal and long-term expansion of SG organoids, containing all differentiated SG cell types. Conversely, Wnt inhibition ablated long-term organoid cultures. Finally, transplantation of cells pre-treated with Wnt agonists into submandibular glands of irradiated mice successfully and robustly restored saliva secretion and increased the number of functional acini in vivo. Collectively, these results identify Wnt signaling as a key driver of adult SG stem cells, allowing extensive in vitro expansion and enabling restoration of SG function upon transplantation.

INTRODUCTION

Tissue homeostasis and regeneration are maintained by resident stem cells that have the ability to self-renew and to generate all differentiated lineages that characterize a particular tissue. Self-renewal of stem cells should be achieved by asymmetric cell division to maintain sufficient numbers of stem cells and allow ample production of mature, functional tissue-specific cells. The balance between self-renewal and differentiation is stringently regulated by cell-intrinsic transcriptional programs and extracellular signals originating from a specialized micro-environment, the stem cell niche (Morrison and Spradling, 2008). Strict cell-extrinsic control is crucial to avoid the continuous self-renewal of stem cells and their possible progression to cancerous cells (Clarke and Fuller, 2006). An important feature of the stem cell niche model is the limited availability of self-renewing factors due to their local release and short signaling distance (Clevers et al., 2014). Understanding the nature of these factors and their effect on adult stem cells has been hindered due to the low abundance of stem cells and the limited number of functional assays.

The salivary gland is a useful model for studying adult stem cell maintenance due to its easy accessibility and extensive regenerative capacity (Ball, 1974; Denny et al., 1993, 1997; Ihrler et al., 2002; Osailan et al., 2006). Salivary glands are complex secretory organs composed of saliva-producing acinar cells, myoepithelial cells which facilitate the saliva expulsion, and ductal cells through which saliva is secreted into the oral cavity (Pringle et al., 2013). Intermingled with ductal cells reside salivary gland stem cells (SGSCs), which express c-Kit, CD49f, CD133, CD24, and CD29 cell-surface markers (Hisatomi et al., 2004; Lombaert et al., 2008a; Nanduri et al., 2011). Upon transplantation, SGSCs attenuate radiation-induced hyposalivation (Lombaert et al., 2008a; Nanduri et al., 2011) and improve tissue homeostasis that is necessary for long-term maintenance of the adult tissue (Nanduri et al., 2013). Although recently we (Nanduri et al., 2014) and others (Xiao et al., 2014) have successfully purified SGSCs able to self-renew and differentiate in vitro and in vivo, the molecular cues underlying the maintenance of SGSCs and the existence of a specialized stem cell niche are still enigmatic.

The canonical Wnt/β-catenin signaling has been shown to play a crucial role in the maintenance of multiple types of adult stem/progenitor cells (Clevers and Nusse, 2012). The Wnt target gene *Lgr5* has been identified as a marker of resident stem cells in the small intestine and colon (Barker et al., 2007), hair follicle (Jaks et al., 2008), stomach (Barker et al., 2010), kidney (Barker et al., 2012), and liver (Huch et al., 2013b). In adult salivary glands, Wnt/β-catenin signaling is weak, but is significantly activated during functional regeneration (Hai et al., 2010).
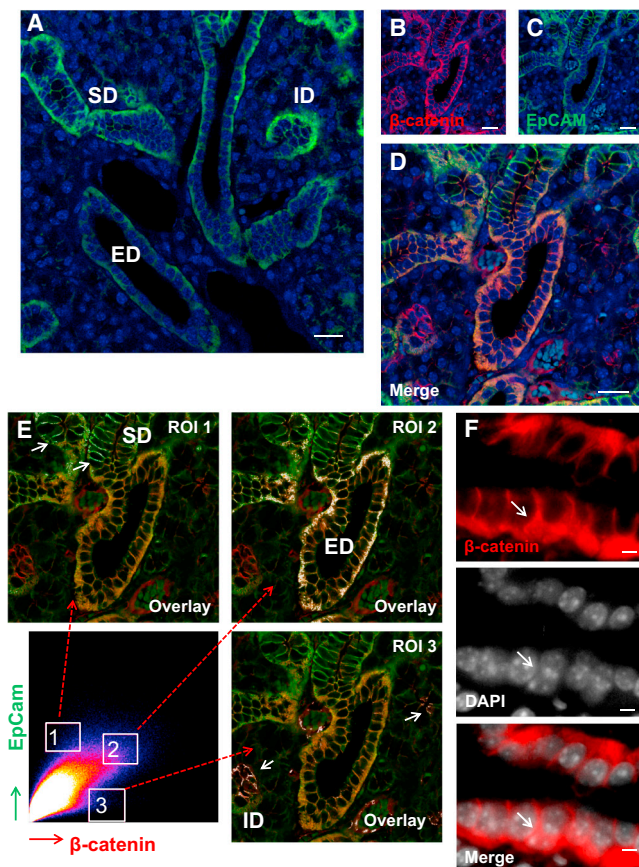
CrossMark

Figure 1. EpCAM-Expressing Ductal Cells Have the Potential to Be Wnt Activated

(A) Immunofluorescence staining of EpCAM in striated (SD), intercalated (ID), and excretory ducts (ED).

(B–D) β-Catenin (red) co-localizes with EpCAM (green) in salivary gland ducts.

(E) Scattergram of co-localization of EpCAM and β-catenin. Different regions of interests (ROI) show which pixels (arrows) are included in the analysis. For each pixel in the fluorescent image, the two intensities (green, red) are used as coordinates in the scattergram. Images analyzed with the ImageJ "Colocalization_Finder" plugin (Christophe Laummonerie; 2006/08/29: Version 1.2).

(F) Nuclear localization of β-catenin in rare basal cells (arrow) of excretory ducts. Top: β-catenin; center: DAPI; bottom: overlay. Scale bars represent 20 μm (A–E) and 5 μm (F).

Furthermore, concurrent transient activation of Wnt/β-catenin signaling ameliorates irradiation-induced salivary gland dysfunction (Hai et al., 2012). Whether Wnt proteins directly control normal SGSC maintenance is still not known. In this study, we used a combination of cell culture and in vivo transplantation experiments to show that Wnt proteins serve as important self-renewing factors for SGSCs.

RESULTS

EpCAM[+] Cells in Salivary Gland Ducts Co-express β-Catenin

In the salivary gland, stem cells have been suggested to reside within the ductal compartment (Denny and Denny, 1999; Man et al., 2001). Therefore, a universal marker for ductal cells of adult submandibular gland would allow identification and enrichment of a population containing stem cells. EpCAM (epithelial cell adhesion molecule) is present on most epithelial cells and has been used as a marker for self-renewing compartments in liver (Dan et al., 2006; Huch et al., 2015) and pancreas (Huch et al., 2013a). To assess the presence of EpCAM in the salivary gland, we stained whole gland sections using immunofluorescence. The expression of EpCAM was detected throughout the whole epithelia of the salivary gland (Figure S1A). However, we encountered most abundant and enhanced expression of EpCAM in the ductal compartment, marking excretory, striated, and intercalated ducts (Figure 1A) and low EpCAM expression in acinar cells, which constitute most of the mouse submandibular gland. No background staining was detected in salivary gland sections treated without primary antibody (Figures S1B and S1D). Interestingly, transcription of EpCAM is activated upon Wnt/β-catenin signaling in other tissues (Yamashita et al., 2007). Therefore, we attempted to determine sites of Wnt signaling in the salivary gland using β-catenin as a general reporter (Peifer et al., 1994). Indeed, highest β-catenin expression was observed to be confined to ductal cells (Figure 1B) of the salivary gland while the acinar cells showed low levels of β-catenin. Again, no background staining was detected without primary antibody (Figures S1C and S1D). Moreover, most cells positive for β-catenin were found to co-express EpCAM (Figures 1C and 1D). To quantify this, we performed co-localization analysis and calculated the Pearson correlation coefficient (PCC) for sub-regions of interest (ROIs). This revealed the strongest correlation of EpCAM and β-catenin occurring in excretory ducts (Figure 1E, ROI 2) (PCC = 0.121644), which were previously suggested to contain the stem cells (Lombaert et al., 2008a; Pringle et al., 2013). Interestingly, striated ducts displayed more exclusive EpCAM^{+} cells (Figure 1E, ROI 1) (PCC = 0.032378) while intercalated ducts revealed more exclusive β-catenin expression (Figure 1E, ROI 3) (PCC = 0.001784). Importantly, scanning of excretory ducts revealed rare basal cells with nuclear β-catenin expression (Figure 1F, arrows), suggesting an occurrence of active Wnt signaling in these cells. The existence of these rare cells agrees with the low level of cell turnover in the salivary glands (Aure et al., 2015).

Recently, Wnt target genes *Lgr5* (Barker et al., 2007) and *Lgr6* (Snippert et al., 2010) were identified as markers of stem cells in the intestine/colon and skin, respectively.
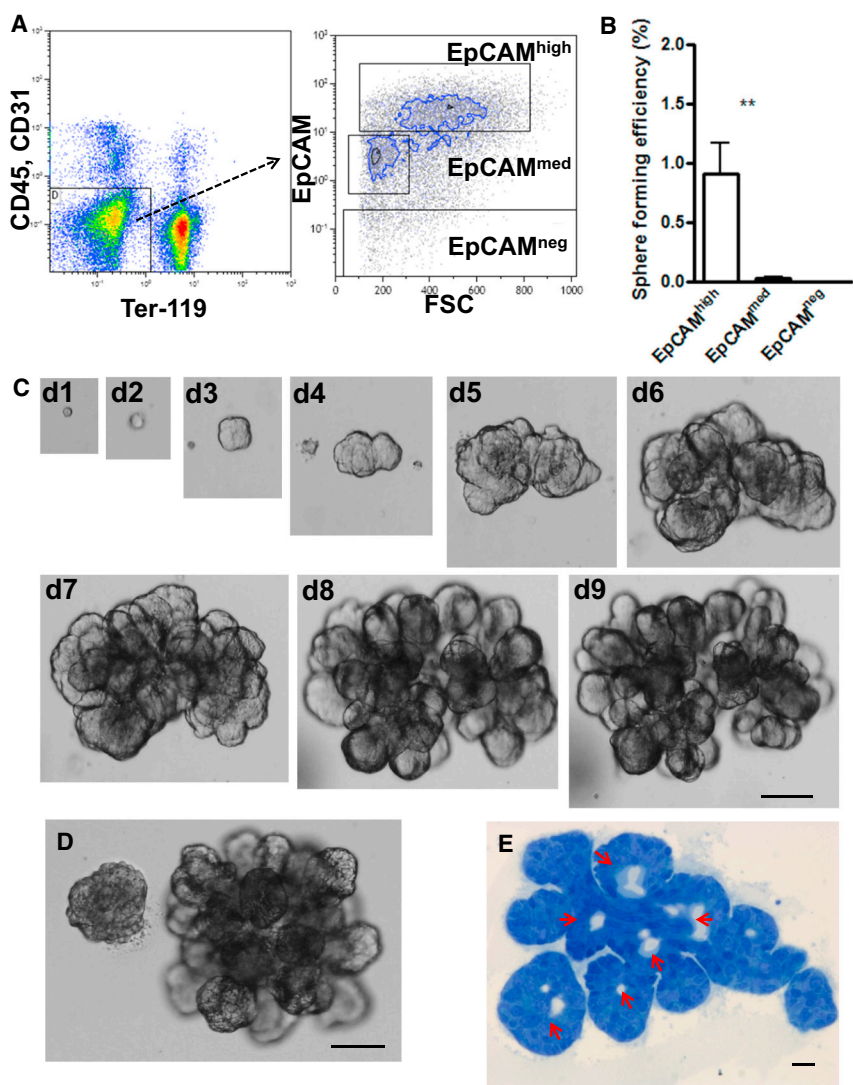
Figure 2. Single EpCAM^high Cells Generate Spheres and Miniglands

(A) Representative FACS gating strategy for the analysis of ductal cells in the salivary gland. Left panel shows the exclusion of lineage marker-expressing cells. Right panel depicts the distribution of EpCAM^high, EpCAM^med, and EpCAM^neg cells in dissociated adult mouse salivary gland. FSC, forward scatter.

(B) Sphere-forming efficiency of EpCAM^high, EpCAM^med, and EpCAM^neg populations (**$p < 0.005$). Data are expressed as the mean ± SEM of three independent experiments.

(C) Differential interference contrast image of a growing minigland until 9 days (d) of culture.

(D) Representative example of a salisphere and a minigland originating from single EpCAM^high in 9-day-old culture.

(E) Toluidine blue staining shows uniform lumen formation throughout minigland (arrows).

Scale bars represent 100 μm (C, D) and 10 μm (E).

We utilized the LGR5-EGFP (Barker et al., 2007) and LGR6-EGFP (Snippert et al., 2010) knockin alleles to determine the expression of LGR5 and LGR6 in the salivary gland. Both receptors are essentially undetectable in the tissue under steady-state conditions (data not shown). This is in line with recent findings in other slow-turnover tissues such as liver (Huch et al., 2013b) and pancreas (Huch et al., 2013a), where under homeostatic conditions no expression of LGR5 was detected. These data indicate that EpCAM^+ cells in salivary gland excretory ducts co-express β-catenin and therefore could potentially be activated by Wnt signaling, albeit not through LGR5/6 receptors.

EpCAM^high Cells Give Rise to Secondary Salivary Gland Spheres and Miniglands

Based on our observations in vivo, we next asked whether Wnt proteins could directly influence EpCAM^+ salivary gland ductal cells in vitro by promoting their sphere-initiating ability. Therefore, salivary glands from adult healthy mice were isolated and digested into single-cell suspension. After removing cell clumps, dead cells, and debris, we depleted CD45^+ and TER119^+ hematopoietic and CD31^+ endothelial cells (Figure 2A). Subsequently, salivary gland cells were subdivided into three distinct cell populations, EpCAM^high, EpCAM^med, and EpCAM^neg, using fluorescence-activated cell sorting (FACS) (Figure 2A). Purified cells were embedded into Matrigel containing enriched medium supplemented with epidermal growth factor (EGF), fibroblast growth factor 2 (FGF2), insulin, and Y-27632 (Nanduri et al., 2014), to which Wnt3a and Rspo1 were added (WRY medium). Under these conditions, 0.9% ± 0.2% of single cells from the EpCAM^high population generated spheres within 24–48 hr (Figure 2B). In contrast, single cells from EpCAM^med and EpCAM^neg populations
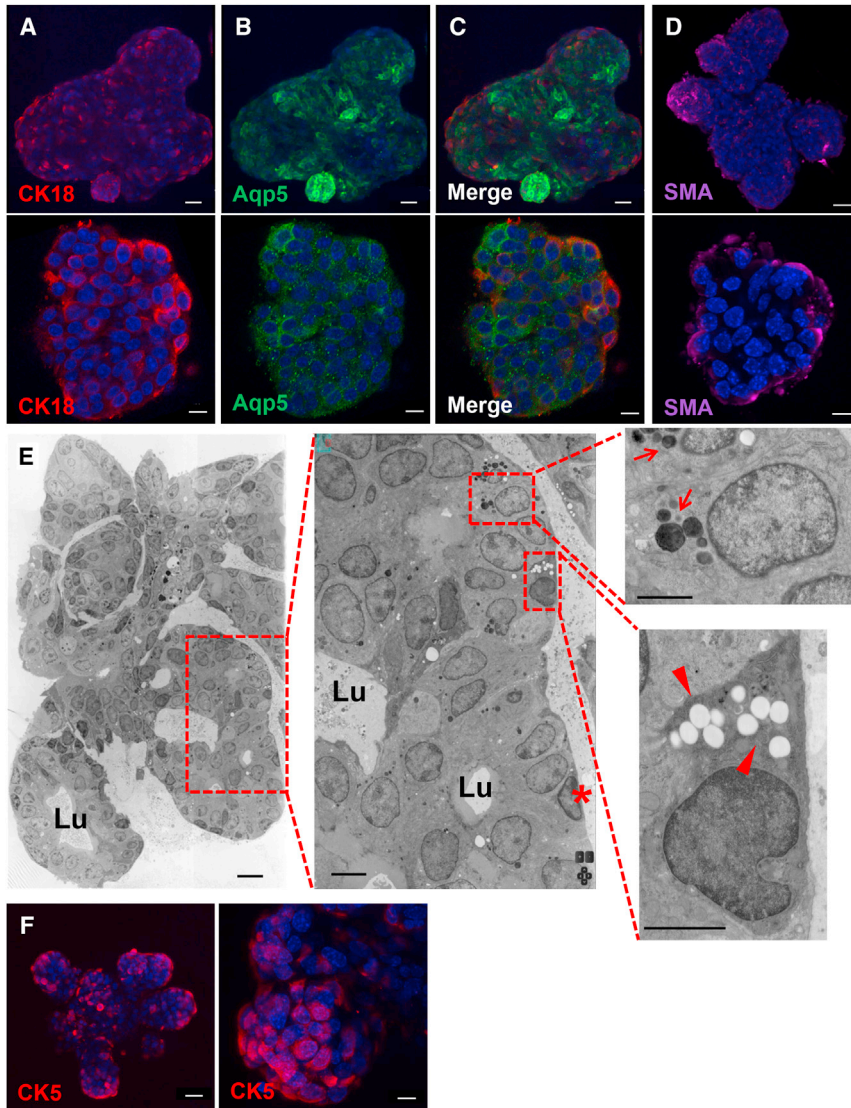
Figure 3. Single-Cell-Derived Miniglands Acquire Fate of Salivary Gland Cells

(A–D) Confocal images (z-stack projection) for salivary gland specific markers. (A) CK18 (red, ductal cells); (B) Aqp5 (green, acinar cells); (C) Overlay of CK18 (red) and Aqp5 (green); (D) α-SMA (purple, myoepithelial cells). Counterstain, Hoechst 33342 (blue).

(E) Electron microscopy demonstrates serous (arrows) and mucous (arrowheads) acinar cells and myoepithelial cells (asterisk). Data are accessible at http://www.nanotomy.org, Salivary gland organoid. Lu, lumen.

(F) Confocal images (z-stack projection) for CK5 (red, embryonic SG progenitor cells). Counterstain, Hoechst 33342 (blue).

Scale bars represent 30 μm (A–D [upper panel], F [left]); 10 μm (A–D [lower panel], F [right]); and 10 μm, 5 μm, and 2 μm in left, center, and right panels of (E), respectively.

were unable to form spheres (<0.05%, Figure 2B). Moreover, only 0.05% ± 0.01% of live, non-marker-selected cells and 0.2% ± 0.1% of non-sorted cells were capable of generating spheres in WRY medium, further indicating that high EpCAM expression pronouncedly enriches for cells with in vitro self-renewing capabilities (Figure S2A). Similarly to gastric organoid units (Barker et al., 2010), supplementing the cultures with either Wnt3a or Rspo1 alone lead to the formation of a lower number of spheres (Figure S2B). We did not observe any cell growth in cultures not supplemented with Wnt proteins (Figure S2B), presumably due to the requirement of Wnt signaling for the initiation of sphere growth under these conditions.

Interestingly, within 9 days of culture 10.8% ± 1.8% of the spheres formed differentiated organoid-like structures, which we termed miniglands (Figures 2C and S2C). Minig-

lands underwent extensive budding events during this time frame, and were up to four to six times bigger than co-cultured salispheres (89.2% ± 1.8%), reaching up to 1 mm in diameter (Figures 2D and S2D) by day 15. Toluidine blue staining of miniglands revealed a lobular structure with evenly distributed lumina (Figure 2E). Moreover, miniglands consisted of differentiated CK18+ ductal (Figures 3A, 3C, and S3A), Aqp5+ acinar (Figures 3B and 3C), and SMA-α+ myoepithelial cells forming the outer layer of a lobe (Figure 3D and Movie S1), as shown by immunostaining, indicative of retention of differentiation potential of EpCAM^high SGSCs in the presence of Wnt agonists. No background staining was detected in any of the samples treated without primary antibody even when enhancing the lasers of the confocal microscope to excessive levels (Figure S3B). Interestingly, ultrastructural analysis of entire

miniglands at high resolution with large-scale electron microscopy (Sokol et al., 2015) further indicated representation of both serous acinar (Figure 3E, arrows) and mucous acinar cells (Figure 3E, arrowheads) as recognized by characteristically electron-dense and electron-pale secretory vesicles, respectively (Movie S2). The basement membrane was lined with myoepithelial cells (Figure 3E, asterisk) distinguished by their elongated shapes. We also observed an abundance of CK5^{+} cells (Figure 3F), which is considered to be a progenitor cell population in embryonic salivary glands (Knox et al., 2010). Taken together, culturing single EpCAM^{high} stem cells in vitro in Wnt-inducing conditions gives rise to three-dimensional structures which (1) consist of all salivary gland cell lineages and (2) contain large numbers of CK5^{+} putative progenitors.

Single Salivary Gland Stem Cell Expansion Is Wnt Driven

Recently we have shown pronounced expansion of SGSCs in vitro in the presence of Rho-kinase inhibitor Y-27632 (Nanduri et al., 2014), without Wnt agonists. However, this expansion was initiated from liquid cultures enriched for primary sphere-forming cells and might involve a paracrine effect of Wnt stimulation. To test the requirement of the Wnt pathway in this format, we isolated salivary glands from adult healthy mice and digested them into dispersed cells, which formed primary salispheres within 3 days (Figure 4A). Next, single cells derived from dissociated primary spheres were embedded in Matrigel supplemented with enriched medium (Figure 4B) (Nanduri et al., 2014) or enriched medium containing a panel of Wnt antagonists: IWR-1-endo (Figure 4D), which stabilizes Axin proteins within the β-catenin destruction complex (Chen et al., 2009), IWP-2 (Figure 4E), which inactivates Porcn, a protein known to be essential for the production of Wnt ligands (Chen et al., 2009), and SFRP-1 (Figure 4F), which directly binds Wnt proteins (Finch et al., 1997). Indeed, chemical inhibition of the Wnt pathway by IWR-1-endo completely suppressed the growth of spheres while treatment with IWP-2 and sFRP1 dramatically reduced the growth of spheres (Figures 4G and 4H). DMSO-treated cells (Figures 4C, 4G, and 4H) did not have a significant effect on the population doublings or sphere-forming efficiency. These data suggest that Wnt signaling is essential for the initiation of sphere growth, not only when isolating SGSCs directly from tissue (Figure 2A) but also in cultures enriched for SGSCs (Lombaert et al., 2008a; Nanduri et al., 2014). We next reasoned that if Wnt inhibition leads to a lack of proliferation in salispheres, Wnt activation may lead to an increased proliferation and salisphere forming potential, and, as such, expansion of the SGSC pool. We tested this by seeding single cells derived from primary salispheres in Matrigel supplemented with WRY medium (Figure 4I).

As expected, the presence of Wnt proteins had an enhanced effect on cell proliferation (population doubling 6.5 ± 0.2) (Figure 4N). Furthermore, we observed a significant effect on sphere-forming efficiency ($15.7\% \pm 1.1\%$) (Figure 4O) when compared with enriched medium conditions (population doubling 3.2 ± 0.2; sphere-forming efficiency $12.0\% \pm 1.0\%$). Disruption of Wnt pathway by IWR-1-endo (Figure 4K), IWP-2 (Figure 4L), or sFRP1 (Figure 4M) in WRY conditions led to a reduced cell growth (3.5 ± 0.1, 0.6 ± 0.2, 1.6 ± 0.4 population doublings, respectively) (Figure 4N) and weakened sphere-forming efficiency ($6.3\% \pm 1.1\%$, $2.0\% \pm 0.6\%$, and $3.3\% \pm 1.2\%$, respectively) (Figure 4O), indicating incomplete inhibition of Wnt signaling by Wnt antagonists in the presence of Wnt3a and R-spondin1. DMSO exposure (Figure 4J) did not alter cell growth or sphere formation (population doubling 5.9 ± 0.3; sphere-forming efficiency $14.3\% \pm 1.9\%$) (Figures 4N and 4O) compared with untreated condition. The self-renewal capacity of cells cultured in WRY conditions was tested by enzymatically by digesting organoids into single cells and plating to a density of 10,000 cells per well, every consecutive week (Figure 4A). The cultures maintained exponential growth for more than 8 months with cell doubling times essentially unchanged during the culturing period (Figure 4P, WRY). Furthermore, when compared with our previously published enriched medium (Figure 4P, EM) (Nanduri et al., 2014), cells grown in the presence of Wnt agonists displayed an enhanced capacity for stem cell expansion.

We then asked whether the original organoids derived from EpCAM^{high} cells (Figure 2) contain cells capable for self-renewal and therefore give rise to long-term SGSC cultures. To this end, salivary glands from adult healthy mice were isolated and digested into single-cell suspension. After removing cell clumps, dead cells, and debris, we depleted CD45^{+} and TER119^{+} hematopoietic and CD31 endothelial cells (Figure S4A). As before, the cells were divided into three cell populations (EpCAM^{high}, EpCAM[med], and EpCAM[neg]) using FACS (Figure S4B) and embedded into Matrigel containing previously defined WRY medium. During 10 days of culture, EpCAM^{high} cells generated organoids (Figure S4C, arrows) as shown previously. As expected, single cells from EpCAM[med] and EpCAM[neg] populations were unable to form organoids (<0.05%) (Figures S4D and S4E). Next, organoids initiated from single EpCAM^{high} cells were dissociated and replated into Matrigel supplemented with WRY medium. Within the period of three passages (3 weeks) these cultures displayed exponential growth (Figure S4F) similar to that of cultures initiated from liquid cultures (Figure 4P). In addition, as cells derived from EpCAM[high] population were passaged, an increase in the ability to form spheres was observed (Figure S4G), indicative of enrichment in stem/progenitor cells when cultured
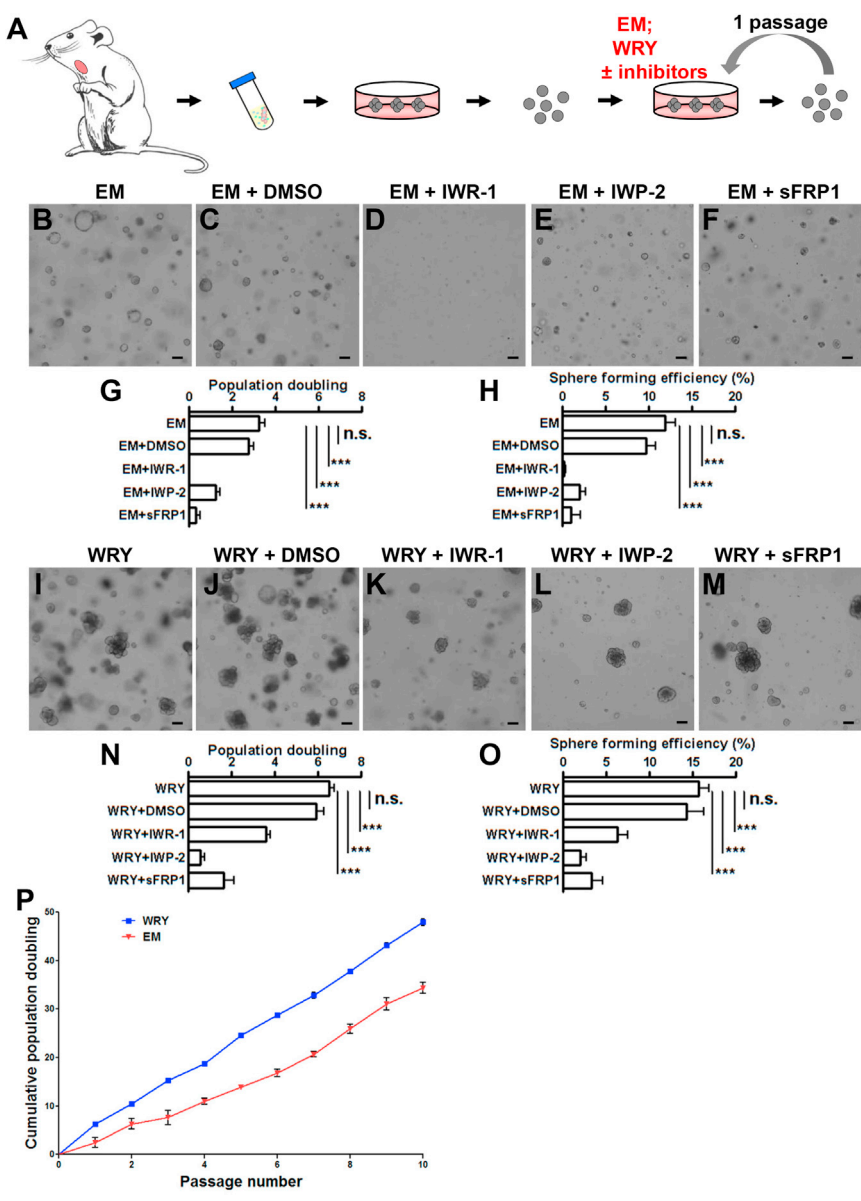
Figure 4. In Vitro Expansion of Salivary Gland Stem Cells

(A) Scheme showing isolation method of SGSCs and establishment of long-term salivary gland organoid culture.

(B–F) Differential interference contrast (DIC) images of salivary gland organoid cultures grown in enriched medium (EM) (B) (Nanduri et al., 2014) in combination with DMSO (C) or Wnt antagonists IWR-1-endo (D), IWP-2 (E), and sFRP1 (F). Scale bars, 100 μm.

(G and H) Population kinetics of salisphere-derived salivary gland organoid cultures during inhibition of Wnt pathway grown in EM representing population doubling (G) and sphere-forming capability (H). ***$p < 0.001$. Data are expressed as the mean ± SEM of three independent experiments. n.s., not significant.

(I–M) DIC images of salivary gland organoid cultures grown in WRY medium (I) in combination with DMSO (J) or Wnt antagonists IWR-1-endo (K), IWP-2 (L), and sFRP1 (M). Scale bars, 100 μm.

(N and O) Population kinetics of salisphere-derived salivary gland organoid cultures during inhibition of Wnt pathway grown in WRY medium representing population doubling (N) and sphere-forming capability (O). ***$p < 0.001$. Data are expressed as the mean ± SEM of three independent experiments. n.s., not significant.

(P) Population dynamics plot of salisphere self-renewal culture (for formula see Experimental Procedures). WRY, minimal media supplemented with Wnt3a, R-spondin1, and y-27632.

Data are expressed as the mean of ± SEM of three independent experiments (G, H, N–P).

under Wnt-inducing conditions. This shows that the EpCAM[high] cell population discerned from freshly isolated salivary glands, in contrast to EpCAM[med] and EpCAM[neg] populations, contains cells with self-renewal potential.

To assess the suitability of expanded SGSCs for in vivo reconstitution experiments, we beforehand tested their tumorigenicity and differentiation potential. First, when transplanting $8 \times 10 \times 10^5$ passage 13 cells subcutaneously into immunocompromised mice, no tumor formation was detected after 1 year in any of the mice analyzed (n = 5) (Figure S5A). Second, when embedding passage 18 spheres into our previously published differentiation assay containing collagen type IV and basement membrane Matrigel

(50%:50%) (Nanduri et al., 2014) the growth of lobular organoids was observed within 14 days (Figure S5B), suggesting a normal differentiation potential when growing salivary gland cells for multiple passages with WR medium. Therefore, we conclude that passaging SGSCs in Wnt-inducing conditions allows massive expansion of the SGSC pool.

Transplantation of Wnt-Induced Cells Unprecedentedly Rescues Irradiation-Damaged Salivary Glands

Based on our in vitro observations showing that only EpCAM^{high} cells give rise to secondary structures indicating
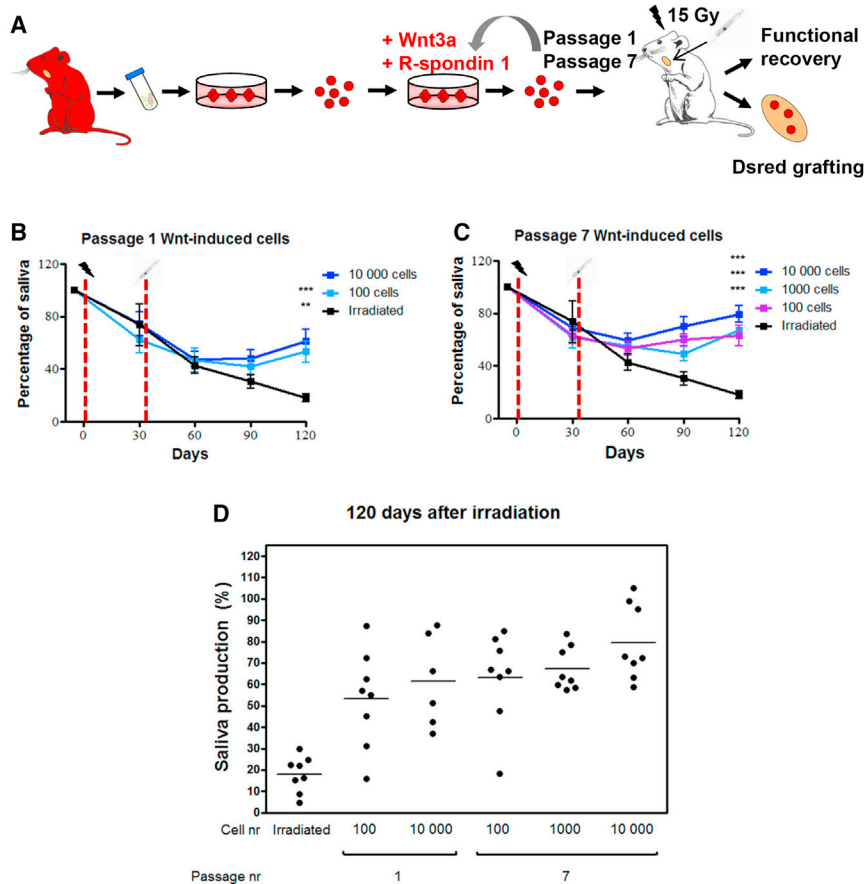
Figure 5. Transplantation of Cultured Wnt-Induced Cells Improves Function of Irradiated Salivary Gland Tissue

(A) Scheme representing the transplantation protocol.

(B) Transplants of 10,000 (blue) and 100 (cyan) passage 1 Wnt-induced cells in time-course analysis of relative saliva production in comparison with irradiated control animals (black). Irradiation time point (left dashed line), transplantation time point (right dashed line). Statistical analysis is shown in comparison with irradiated control group (***p < 0.001, **p < 0.01 at relevant time points). Data are expressed as the mean ± SEM, n = 8 animals per time point.

(C) Transplants of 10,000 (blue), 1,000 (purple), and 100 (cyan) passage 7 Wnt-induced cells in time-course analysis of relative saliva production in comparison with irradiated control animals (black). Statistical analysis is shown in comparison with irradiated control group (***p < 0.001 at relevant time points). Data are expressed as the mean ± SEM, n = 8 animals per time point.

(D) Relative saliva production at 120 days after irradiation in animals transplanted with 100 and 10,000 passage 1, or 100, 1,000, and 10,000 passage 7 Wnt-induced cells per animal. Each data point represents a recipient animal. Note the uniform response of animals transplanted with passage 7 Wnt-induced cells.

the presence of stem cells, we finally tested the potential of these cells to rescue radiation-induced hyposalivation in vivo. For this purpose ACTB-DsRed (dsRed) mice were used as donor to enable tracing of the donor cells after transplantation. First, sphere cultures from dsRed mice were initiated and cultured for one or seven passages in basement membrane Matrigel supplemented with WR media (Figure 5A). Subsequently, cultures were collected, trypsinized into single-cell suspension, and transplanted intraglandularly into C57BL/6 recipient mice, which were previously locally irradiated with 15 Gy to the head and neck region (Lombaert et al., 2008a). Both glands in each mouse received equal cell numbers, so that a total cell number of 100, 1,000, or 10,000 were transplanted per recipient mouse. The functionality of the transplanted glands was determined by pilocarpine-stimulated saliva flow rate, as described previously (Lombaert et al., 2008a). As expected, 120 days after irradiation, saliva production dropped to 17% ± 3% of pre-irradiation values (Figures 5B–5D) in control animals (irradiated and non-transplanted). In contrast, saliva flow of mice transplanted with 100 or 10,000 passage 1 Wnt-induced cells increased significantly to 53% ± 8% and 62% ± 9%, respectively (Figures 5B and 5D). Furthermore, the transplantation was even more successful in mice transplanted with 100, 1,000 or 10,000 passage 7 Wnt-induced cells, reaching levels of 63% ± 8%, 67% ± 3%, and 79% ± 6% of pre-irradiation saliva flow, respectively (Figures 5C and 5D). This indicates that our culturing conditions are optimized for the enrichment of the SGSC pool with in vivo reconstitution ability.

Recovery of the glandular tissue was further demonstrated by improvement of general morphology (Figures 6A–6C) and the reappearance of functional acinar tissue (Figures 6A–6C, asterisk). The histological improvement was observed in all transplanted mice when compared with irradiated controls (Figure 6D), returning to levels close to non-irradiated controls determined by strong increase in acini (Figure 6E). We also analyzed the engraftment of Wnt-induced cells by dsRed staining on serial sections of the entire salivary gland. We found dsRed+ ducts (Figure 6F, arrows) and acini (Figure 6F, arrowheads) incorporated in the tissue, indicating that they were derived
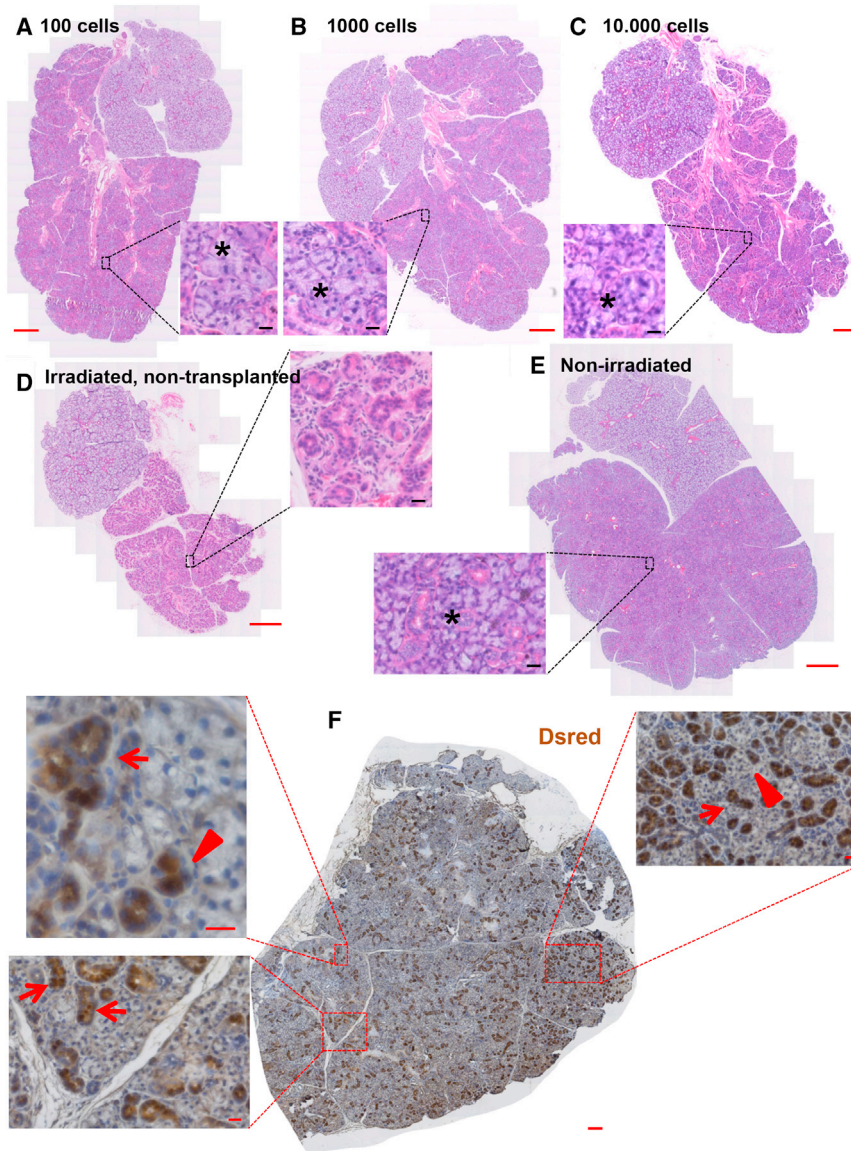
Figure 6. Donor-Derived Cells Regenerate Destroyed Salivary Gland Tissue

(A–E) H&E staining of SG tissue irradiated and transplanted with 100 (A), 1,000 (B) or 10,000 (C) Wnt-induced cells, irradiated control (D), and untreated control (E), showing presence of acini (asterisk).

(F) Immunohistochemical staining for DsRed reveals incorporation of transplanted Wnt-induced cells into donor tissue and formation of ducts (arrows) and acini (arrowheads).

Scale bars represent 100 μm (zoom-out panels) and 20 μm (zoom-in panels).

from donor cells. No specific staining was detected in C57BL/6 salivary gland sections treated with dsRed antibody (Figure S5A) while most of the cells were positively stained in salivary gland sections of dsRed mice (Figure S5B). We did not observe any sign of tumor growth or dysplastic change in any of the transplanted areas, indicating the non-transformed origin of cultured cells. Taken together, these data reveal that culturing SGSCs in Wnt-inducing conditions broadly expands SGSCs with enhanced potential to restore functionality in destroyed submandibular glands. However, with these experiments we cannot sufficiently conclude that Wnt proteins are responsible for restoring the function of irradiated salivary glands in vivo.

DISCUSSION

Wnt/β-catenin signaling is involved in many biological processes, including proliferation, differentiation, organogenesis, and cell migration (Clevers and Nusse, 2012). It has been shown previously that combinations of Wnt and R-spondin proteins support long-term cultures of small intestine (Sato et al., 2009), stomach (Barker et al., 2010), liver (Huch et al., 2013b), and pancreas (Huch et al., 2013a). Until now, the role of Wnt signaling on key properties of SGSC regulation has remained elusive. In this study, we provide evidence that Wnt proteins are required for SGSC self-renewal and robustly promote their long-term expansion in culture. Our study further strengthens the role of Wnt

signaling as a universal self-renewal pathway (Lim et al., 2013; Reya et al., 2003; Zeng and Nusse, 2010).

A lack of stem cell assays in the adult salivary gland field has hindered studies aimed at assessing functional properties and/or regenerative potential of putative stem cell populations. Our previous attempts for studying SGSC biology were based on in vitro cultures, already enriched for stem/progenitor cells (Lombaert et al., 2008a; Nanduri et al., 2014). Here we report the development of an optimized culture system for generating salivary gland organoids from primary adult submandibular glands in vitro, based on activation of Wnt signaling. Although in addition to the common transmembrane expression of EpCAM we also detect an unexpected basal localization of the protein in excretory duct cells of the salivary gland, FACS selection for single EpCAM^{high} cells and subsequent culturing in the presence of Wnt-activating proteins efficiently generate three-dimensional salivary gland organoids that closely resemble primary salivary gland tissue.

Recently, Xiao et al. (2014) successfully isolated and cultured Lin$^-$CD24$^+$c-Kit$^+$Sca1$^+$ SGSCs as spheres lacking the phenotypical hallmark of differentiation: branching morphogenesis. Contrary to this, the organoids presented here underwent a series of budding events, until reaching sizes up to 1 mm (Figure S2C). Combined with orthotopic transplantation (Ogawa et al., 2013), these findings may open up novel routes to organ-replacement regenerative therapy. Using the technique reported here we are able to expand SGSCs, derived from a single animal, to clinically relevant numbers without the use of specific stem cell markers. Previously reported methods have been required to start expansion cultures with cells derived from multiple animals, and used cell-surface markers that are mouse specific (Xiao et al., 2014), rendering the expansion protocol less clinically relevant.

Achieving control of cell fate determination in adult tissues is one of the key goals of regenerative medicine. Given the central role of Wnt-mediated cellular responses in stem cell self-renewal, we focused our attention on activation as well as inhibition of Wnt signaling. By using a panel of chemical inhibitors of the Wnt pathway, we effectively show that Wnt signaling is required for the maintenance of SGSC cultures. Although the ability of IWR and IWP compounds to selectively inhibit the Wnt pathway has been characterized elsewhere (Chen et al., 2009), it is still possible that chemical inhibition causes off-target effects. Therefore, in the future it would be of interest to use a conditional β-catenin loss-of-function mouse model (Huelsken et al., 2001) or the CRISPR-Cpf1 genome editing system (Zetsche et al., 2015) for the ablation of Wnt pathway.

Ultimately, this study provides proof of principle that SGSCs cultured under Wnt-inducing conditions can be used for stem cell therapy to irradiation-damaged epithe-lium and possibly other cases of salivary gland dysfunction. Remarkably, the transplanted cells adhere and engraft into damaged tissue and contribute to the normal homeostasis of the salivary gland. We report an unprecedented improvement of saliva flow recovery over previously reported methods (Lombaert et al., 2008b; Nanduri et al., 2011, 2014; Xiao et al., 2014), which could have been achieved by transplantation of a heterogeneous pool of cells containing stem, progenitor, and differentiated cells present in these cultures. Although translation to the human situation is needed, the current study implies that in vitro expansion and transplantation of long-term cultured SGSCs may be a promising option for patients with severe salivary gland hypofunction.

In conclusion, we provide clear evidence that Wnt signals are necessary for SGSC maintenance in vitro. However, this does not exclude the relevance of other pathways in these processes. For example, platelet-derived growth factor receptor signaling, in concert with fibroblast growth factor signaling, has been shown to be essential for proliferation and survival of ex vivo cultures of embryonic salivary gland progenitors (Steinberg et al., 2005; Yamamoto et al., 2008). Furthermore, EGFs and their receptors are important for embryonic salivary gland proliferation (Haara et al., 2009; Knox et al., 2010). However, none of these pathways have exploited to study adult stem cell maintenance in vitro to the extent as the Wnt-signaling pathway presented here. We believe that the efficient in vitro system reported here will be of vital use for validating and implementing further studies on adult SGSC biology and for the discovery of novel pathways involved in the maintenance and regeneration of salivary glands.

EXPERIMENTAL PROCEDURES

Mice
Eight- to 12-week-old female C57BL/6 mice were purchased from Harlan. NOD.Cg-$Prkdc^{scid}Il2rg^{tm1Wjl}$/SzJ, B6.Cg-Tg(ACTB-DsRed*MST)1Nagy/J, and B6.129P2-$Lgr5^{tm1(cre/ESR1)Cle}$/J animals were bred in the Central Animal Facility of University Medical Center, Groningen. LGR6-EGFP (Snippert et al., 2010) were bred in the Hubrecht Institute, University Medical Center Utrecht. The mice were maintained under conventional conditions and fed ad libitum with food pellets (RMH-B; Hope Farms) and water. All experiments were approved by the Ethical Committee on animal testing of the University of Groningen.

Immunostaining
Mouse salivary glands were 4% formaldehyde fixed (24 hr at room temperature) and processed for paraffin embedding. Following dehydration, the tissue was embedded in paraffin and sliced into 5-μm sections. The sections were dewaxed, boiled for 8 min in pre-heated 10 mM citric acid retrieval buffer (pH 6.0) containing 0.05% Tween 20, washed thoroughly prior to primary antibody

exposure, and labeled for the following markers: EpCAM (1:100; Schnell et al., 2013), β-catenin (1:100; Transduction Laboratories, 610154), and dsRed (1:100; BioVision, #3984-100). For fluorescence microscopy, Alexa Fluor 488 goat anti-rabbit (Life Technologies, A11008) or Alexa Fluor 594 donkey anti-mouse (Life Technologies, A21203) conjugates at 1:300 dilution were used as secondary antibodies. Nuclear staining was performed with DAPI (Sigma-Aldrich). H&E staining was performed according to standard protocols. Visualization for bright-field microscopy was accomplished by addition of specific secondary biotin-carrying antibodies (Dako), an avidin-biotin-horseradish peroxidase complex (ELITE ABC Kit, Vector Laboratories) and the diaminobenzidine chromogen. Nuclear staining was performed with hematoxylin.

Cell Sorting and Single-Cell Salivary Gland Sphere Culture

Salivary glands were harvested from healthy adult mice, and mechanically disrupted by a gentleMACS Dissociator (Milteny) followed by enzymatic digestion with collagenase type II (0.63 mg/ml; Gibco), hyaluronidase (0.5 mg/ml; Sigma-Aldrich), and $CaCl_2$ (6.25 mM; Sigma-Aldrich). After filtering through a 100-μm cell strainer the suspension was dissociated using 0.05% trypsin-EDTA (Gibco) following filtering through a 35-μm strainer. Cell pellets were incubated with anti-mouse CD31-PE (eBioscience, 12-0311-82), CD45-PE (Biolegend, 103106), TER-119-PE/Cy7 (Biolegend, 116222), and EpCAM-APC antibody (eBioscience, 17-5791-80) for 15 min at room temperature. After washing thoroughly, cells were suspended in a solution containing propidium iodide (PI; 1 mg/ml; Sigma-Aldrich), $MgSO_4$ (10 mM; Sigma-Aldrich), and DNase I (50 μg/ml; Sigma-Aldrich). Pulse-width gating excluded cell doublets while dead cells were excluded by gating on PI-negative cells. Positive gating was based on the comparison of non-stained and single antibody-stained samples. Sorted cells were embedded in basement membrane Matrigel (BD Biosciences) and seeded in 12 wells. Cells were cultured in enriched medium (Nanduri et al., 2014) or WRY medium (DMEM/F12 containing Pen/Strep antibiotics [1×; Invitrogen], Glutamax [1×; Invitrogen], N2 [1×; Gibco], EGF [20 ng/ml; Sigma-Aldrich], FGF2 [20 ng/ml; Sigma-Aldrich], insulin [10 μg/ml; Sigma-Aldrich], dexamethasone [1 μM; Sigma-Aldrich], Y-27632 [10 μM; Sigma-Aldrich], 10% R-spondin1 conditioned medium [provided by C. Kuo], and 50% Wnt3a conditioned medium).

Primary salispheres were cultured as published previously (Lombaert et al., 2008a). In brief, cell suspensions were prepared first by mechanical disruption with gentleMACS (Milteny) followed by enzymatic digestion with collagenase type II (0.63 mg/ml; Gibco), hyaluronidase (0.5 mg/ml; Sigma-Aldrich), and $CaCl_2$ (6.25 mM; Sigma-Aldrich). After washing thoroughly, cell suspensions were resuspended in DMEM/F12 medium containing 1× Pen/Strep antibiotics (Invitrogen), Glutamax (1×; Invitrogen), EGF (20 ng/ml; Sigma-Aldrich), FGF2 (20 ng/ml; Sigma-Aldrich), N2 (1×; Gibco), insulin (10 μg/ml; Sigma-Aldrich), and dexamethasone (1 μM; Sigma-Aldrich), at a density of 400,000 cells per well of a 12-well plate.

Self-Renewal Assay

Three-day salisphere cultures were dispersed to single-cell suspensions using 0.05% trypsin-EDTA (Invitrogen), enumerated and

concentration adjusted to 0.4×10^6 cells/ml. 25 μl of cell suspension was combined on ice with 50 μl of BM Matrigel and deposited in the center of 12-well tissue culture plates. After solidifying the gels for 20 min at 37°C, gels were covered in minimal medium (MM), enriched medium (Nanduri et al., 2014), WR medium, WRY medium, or combinations of enriched medium or WRY medium containing Wnt antagonists IWR-1-endo (20 μM, Cayman Chemical), IWP-2 (1 μM, Merck Millipore), or sFRP1 (20 ng/ml, Peprotech). 7–10 days after seeding, Matrigel was dissolved by incubation with Dispase (1 mg/ml; Sigma) for 1 hr at 37°C. Spheres released from the gels were processed to a single-cell suspension using 0.05% trypsin-EDTA, cell number and sphere number noted, and encapsulation in Matrigel repeated. This cycle was repeated up to 25 times (25 passages). Cell numbers seeded at the start of each passage and harvested at the end were used to calculate the number of population doublings that had occurred, using the following formula, where pd is population doublings and ln is natural log.

$$pd = \frac{ln\ (harvested\ cells / seeded\ cells\ )}{ln2}.$$

Whole-Mount Immunostaining

Matrigel in 10-day salisphere culture was dissolved by incubation with Dispase for 1 hr at 37°C. Released spheres and miniglands were FA fixed for 12 hr at 4°C, washed thoroughly, and labeled for the following markers: Aqp5 (1.5 μg/ml; Alomone Labs, AQP-005), CK18 (1:100; Abcam, ab668), α-SMA (1:100; Sigma-Aldrich, A2547), and CK5 (1:100; Covance, PRB-160P). Alexa Fluor 488 goat anti-rabbit (Life Technologies, A11008) or Alexa Fluor 594 donkey anti-mouse (Life Technologies, A21203) conjugates at 1:300 dilution were used as secondary antibodies. Nuclear counterstaining was performed with Hoechst 33,258 (Sigma-Aldrich).

Transmission Electron Microscopy

Large-scale electron microscopic analysis was carried out essentially as described by Sokol et al. (2015). Ten-day salisphere culture in Matrigel was fixed in 2% glutaraldehyde in 0.1 M sodium cacodylate buffer for 24 hr at 4°C. After fixation in 1% osmium tetroxide/1.5% potassium ferrocyanide (2 hr at 4°C), salispheres were dehydrated using ethanol and embedded in EPON epoxy resin. 60-nm sections were cut and contrasted using 2% uranyl acetate in methanol followed by Reynolds lead citrate. Images were taken with a Zeiss Supra55 in STEM mode at 29 kV using an external scan generator (Fibics) yielding mosaics of large-area scans at 2-nm pixel resolution. These large-scale TIFF images were stitched and converted to html files using VE Viewer (Fibics). These html files can be opened via the link http://www.nanotomy.org, Salivary gland organoid. Annotations were done on the original TIFF files using Adobe Photoshop.

Irradiation and Regeneration Assay

The irradiation and regeneration assay employed here was described earlier (Lombaert et al., 2008a). In brief, salivary glands of female C57BL/6 mice were irradiated with a single dose of 15 Gy (Precision X-Ray). Four weeks after irradiation, mice were anesthetized and salivary gland was exposed by a small incision.

As a source of donor cells, passage 1 or passage 7 Wnt-induced or non-induced salisphere cultures were dissociated into single-cell solution, 100, 1,000, or 10,000 cells suspended in equal volumes of α-MEM (Gibco) and injected intraglandularly into both SMGs of irradiated mice. Saliva was collected for 15 min at 30, 60, 90, and 120 days after irradiation.

Image Analysis

Immunofluorescence images from tissue sections and images of cultivated cells were acquired with a Leica TCS Sp8 confocal microscope. Images of time-lapse experiments were acquired with an Olympus IMT-2 inverted microscope. Immunohistochemical images of tissue sections were acquired with a Leica 6000 series microscope or a Tissuegnostics TissueFAXS high-throughput fluorescence microscope. Co-localization of two proteins was quantified by the ImageJ "Colocalization_Finder" plugin (Christophe Laummonerie 2006/08/29: Version 1.2). Immunofluorescence images were reconstructed and analyzed using Imaris (Bitplane) software.

Data Analysis

All values are represented as mean ± SEM. A two-way ANOVA and Bonferroni post hoc test with α values of 0.05 were applied to the time-course analysis of saliva flow. Numbers (n) for tested groups are stated in the figure legends. All calculations were performed using GraphPad Prism software.

SUPPLEMENTAL INFORMATION

Supplemental Information includes six figures and two movies and can be found with this article online at http://dx.doi.org/10.1016/j.stemcr.2015.11.009.

REFERENCES

Aure, M.H., Konieczny, S.F., and Ovitt, C.E. (2015). Salivary gland homeostasis is maintained through acinar cell self-duplication. Dev. Cell. *33*, 231–237.

Ball, W.D. (1974). Development of the rat salivary glands. 3. Mesenchymal specificity in the morphogenesis of the embryonic submaxillary and sublingual glands of the rat. J. Exp. Zool. *188*, 277–288.

Barker, N., van Es, J.H., Kuipers, J., Kujala, P., van den Born, M., Cozijnsen, M., Haegebarth, A., Korving, J., Begthel, H., Peters, P.J., et al. (2007). Identification of stem cells in small intestine and colon by marker gene Lgr5. Nature *449*, 1003–1007.

Barker, N., Huch, M., Kujala, P., van de Wetering, M., Snippert, H.J., van Es, J.H., Sato, T., Stange, D.E., Begthel, H., van den Born, M., et al. (2010). Lgr5(+ve) stem cells drive self-renewal in the stomach and build long-lived gastric units in vitro. Cell Stem Cell *6*, 25–36.

Barker, N., Rookmaaker, M.B., Kujala, P., Ng, A., Leushacke, M., Snippert, H., van de Wetering, M., Tan, S., Van Es, J.H., Huch, M., et al. (2012). Lgr5(+ve) stem/progenitor cells contribute to nephron formation during kidney development. Cell Rep. *2*, 540–552.

Chen, B., Dodge, M.E., Tang, W., Lu, J., Ma, Z., Fan, C.W., Wei, S., Hao, W., Kilgore, J., Williams, N.S., et al. (2009). Small molecule-mediated disruption of Wnt-dependent signaling in tissue regeneration and cancer. Nat. Chem. Biol. *5*, 100–107.

Clarke, M.F., and Fuller, M. (2006). Stem cells and cancer: two faces of eve. Cell *124*, 1111–1115.

Clevers, H., and Nusse, R. (2012). Wnt/beta-catenin signaling and disease. Cell *149*, 1192–1205.

Clevers, H., Loh, K.M., and Nusse, R. (2014). Stem cell signaling. An integral program for tissue renewal and regeneration: Wnt signaling and stem cell control. Science *346*, 1248012.

Dan, Y.Y., Riehle, K.J., Lazaro, C., Teoh, N., Haque, J., Campbell, J.S., and Fausto, N. (2006). Isolation of multipotent progenitor cells from human fetal liver capable of differentiating into liver and mesenchymal lineages. Proc. Natl. Acad. Sci. USA *103*, 9912–9917.

Denny, P.C., and Denny, P.A. (1999). Dynamics of parenchymal cell division, differentiation, and apoptosis in the young adult female mouse submandibular gland. Anat. Rec. *254*, 408–417.

Denny, P.C., Chai, Y., Klauser, D.K., and Denny, P.A. (1993). Parenchymal cell proliferation and mechanisms for maintenance of granular duct and acinar cell populations in adult male mouse submandibular gland. Anat. Rec. *235*, 475–485.

Denny, P.C., Ball, W.D., and Redman, R.S. (1997). Salivary glands: a paradigm for diversity of gland development. Crit. Rev. Oral Biol. Med. *8*, 51–75.

Finch, P.W., He, X., Kelley, M.J., Uren, A., Schaudies, R.P., Popescu, N.C., Rudikoff, S., Aaronson, S.A., Varmus, H.E., and Rubin, J.S. (1997). Purification and molecular cloning of a secreted, frizzled-related antagonist of Wnt action. Proc. Natl. Acad. Sci. USA *94*, 6770–6775.

Haara, O., Koivisto, T., and Miettinen, P.J. (2009). EGF-receptor regulates salivary gland branching morphogenesis by supporting proliferation and maturation of epithelial cells and survival of mesenchymal cells. Differentiation *77*, 298–306.

Hai, B., Yang, Z., Millar, S.E., Choi, Y.S., Taketo, M.M., Nagy, A., and Liu, F. (2010). Wnt/beta-catenin signaling regulates postnatal development and regeneration of the salivary gland. Stem Cell Dev. *19*, 1793–1801.

Hai, B., Yang, Z., Shangguan, L., Zhao, Y., Boyer, A., and Liu, F. (2012). Concurrent transient activation of Wnt/beta-catenin pathway prevents radiation damage to salivary glands. Int. J. Radiat. Oncol. Biol. Phys. *83*, e109–e116.

Hisatomi, Y., Okumura, K., Nakamura, K., Matsumoto, S., Satoh, A., Nagano, K., Yamamoto, T., and Endo, F. (2004). Flow cytometric isolation of endodermal progenitors from mouse salivary gland differentiate into hepatic and pancreatic lineages. Hepatology *39*, 667–675.

Huch, M., Bonfanti, P., Boj, S.F., Sato, T., Loomans, C.J., van de Wetering, M., Sojoodi, M., Li, V.S., Schuijers, J., Gracanin, A., et al. (2013a). Unlimited in vitro expansion of adult bi-potent pancreas progenitors through the Lgr5/R-spondin axis. EMBO J. *32*, 2708–2721.

Huch, M., Dorrell, C., Boj, S.F., van Es, J.H., Li, V.S., van de Wetering, M., Sato, T., Hamer, K., Sasaki, N., Finegold, M.J., et al. (2013b). In vitro expansion of single Lgr5+ liver stem cells induced by Wnt-driven regeneration. Nature *494*, 247–250.

Huch, M., Gehart, H., van Boxtel, R., Hamer, K., Blokzijl, F., Verstegen, M.M., Ellis, E., van Wenum, M., Fuchs, S.A., de Ligt, J., et al. (2015). Long-term culture of genome-stable bipotent stem cells from adult human liver. Cell *160*, 299–312.

Huelsken, J., Vogel, R., Erdmann, B., Cotsarelis, G., and Birchmeier, W. (2001). beta-Catenin controls hair follicle morphogenesis and stem cell differentiation in the skin. Cell *105*, 533–545.

Ihrler, S., Zietz, C., Sendelhofert, A., Lang, S., Blasenbreu-Vogt, S., and Lohrs, U. (2002). A morphogenetic concept of salivary duct regeneration and metaplasia. Virchows Arch. *440*, 519–526.

Jaks, V., Barker, N., Kasper, M., van Es, J.H., Snippert, H.J., Clevers, H., and Toftgard, R. (2008). Lgr5 marks cycling, yet long-lived, hair follicle stem cells. Nat. Genet. *40*, 1291–1299.

Knox, S.M., Lombaert, I.M., Reed, X., Vitale-Cross, L., Gutkind, J.S., and Hoffman, M.P. (2010). Parasympathetic innervation maintains epithelial progenitor cells during salivary organogenesis. Science *329*, 1645–1647.

Lim, X., Tan, S.H., Koh, W.L., Chau, R.M., Yan, K.S., Kuo, C.J., van Amerongen, R., Klein, A.M., and Nusse, R. (2013). Interfollicular epidermal stem cells self-renew via autocrine Wnt signaling. Science *342*, 1226–1230.

Lombaert, I.M., Brunsting, J.F., Wierenga, P.K., Faber, H., Stokman, M.A., Kok, T., Visser, W.H., Kampinga, H.H., de Haan, G., and Coppes, R.P. (2008a). Rescue of salivary gland function after stem cell transplantation in irradiated glands. PLoS One *3*, e2063.

Lombaert, I.M., Brunsting, J.F., Wierenga, P.K., Kampinga, H.H., de Haan, G., and Coppes, R.P. (2008b). Cytokine treatment improves parenchymal and vascular damage of salivary glands after irradiation. Clin. Cancer Res. *14*, 7741–7750.

Man, Y.G., Ball, W.D., Marchetti, L., and Hand, A.R. (2001). Contributions of intercalated duct cells to the normal parenchyma of submandibular glands of adult rats. Anat. Rec. *263*, 202–214.

Morrison, S.J., and Spradling, A.C. (2008). Stem cells and niches: mechanisms that promote stem cell maintenance throughout life. Cell *132*, 598–611.

Nanduri, L.S., Maimets, M., Pringle, S.A., van der Zwaag, M., van Os, R.P., and Coppes, R.P. (2011). Regeneration of irradiated salivary glands with stem cell marker expressing cells. Radiother. Oncol. *99*, 367–372.

Nanduri, L.S., Lombaert, I.M., van der Zwaag, M., Faber, H., Brunsting, J.F., van Os, R.P., and Coppes, R.P. (2013). Salisphere derived c-Kit+ cell transplantation restores tissue homeostasis in irradiated salivary gland. Radiother. Oncol. *108*, 458–463.

Nanduri, L.S., Baanstra, M., Faber, H., Rocchi, C., Zwart, E., de Haan, G., van Os, R., and Coppes, R.P. (2014). Purification and ex vivo expansion of fully functional salivary gland stem cells. Stem Cell Rep. *3*, 957–964.

Ogawa, M., Oshima, M., Imamura, A., Sekine, Y., Ishida, K., Yamashita, K., Nakajima, K., Hirayama, M., Tachikawa, T., and Tsuji, T. (2013). Functional salivary gland regeneration by transplantation of a bioengineered organ germ. Nat. Commun. *4*, 2498.

Osailan, S.M., Proctor, G.B., Carpenter, G.H., Paterson, K.L., and McGurk, M. (2006). Recovery of rat submandibular salivary gland function following removal of obstruction: a sialometrical and sialochemical study. Int. J. Exp. Pathol. *87*, 411–423.

Peifer, M., Sweeton, D., Casey, M., and Wieschaus, E. (1994). wingless signal and Zeste-white 3 kinase trigger opposing changes in the intracellular distribution of Armadillo. Development *120*, 369–380.

Pringle, S., Van Os, R., and Coppes, R.P. (2013). Concise review: adult salivary gland stem cells and a potential therapy for xerostomia. Stem Cells *31*, 613–619.

Reya, T., Duncan, A.W., Ailles, L., Domen, J., Scherer, D.C., Willert, K., Hintz, L., Nusse, R., and Weissman, I.L. (2003). A role for Wnt signalling in self-renewal of haematopoietic stem cells. Nature *423*, 409–414.

Sato, T., Vries, R.G., Snippert, H.J., van de Wetering, M., Barker, N., Stange, D.E., van Es, J.H., Abo, A., Kujala, P., Peters, P.J., et al. (2009). Single Lgr5 stem cells build crypt-villus structures in vitro without a mesenchymal niche. Nature *459*, 262–265.

Schnell, U., Kuipers, J., Mueller, J.L., Veenstra-Algra, A., Sivagnanam, M., and Giepmans, B.N. (2013). Absence of cell-surface EpCAM in congenital tufting enteropathy. Hum. Mol. Genet. *22*, 2566–2571.

Snippert, H.J., Haegebarth, A., Kasper, M., Jaks, V., van Es, J.H., Barker, N., van de Wetering, M., van den Born, M., Begthel, H., Vries, R.G., et al. (2010). Lgr6 marks stem cells in the hair follicle that generate all cell lineages of the skin. Science *327*, 1385–1389.

Sokol, E., Kramer, D., Diercks, G.F., Kuipers, J., Jonkman, M.F., Pas, H.H., and Giepmans, B.N. (2015). Large-scale electron microscopy maps of patient skin and mucosa provide insight into pathogenesis of blistering diseases. J. Invest. Dermatol. *135*, 1763–1770.

Steinberg, Z., Myers, C., Heim, V.M., Lathrop, C.A., Rebustini, I.T., Stewart, J.S., Larsen, M., and Hoffman, M.P. (2005). FGFR2b signaling regulates ex vivo submandibular gland epithelial cell proliferation and branching morphogenesis. Development *132*, 1223–1234.

Xiao, N., Lin, Y., Cao, H., Sirjani, D., Giaccia, A.J., Koong, A.C., Kong, C.S., Diehn, M., and Le, Q.T. (2014). Neurotrophic factor GDNF promotes survival of salivary stem cells. J. Clin. Invest. *124*, 3364–3377.

Yamamoto, S., Fukumoto, E., Yoshizaki, K., Iwamoto, T., Yamada, A., Tanaka, K., Suzuki, H., Aizawa, S., Arakaki, M., Yuasa, K., et al. (2008). Platelet-derived growth factor receptor regulates salivary gland morphogenesis via fibroblast growth factor expression. J. Biol. Chem. *283*, 23139–23149.

Yamashita, T., Budhu, A., Forgues, M., and Wang, X.W. (2007). Activation of hepatic stem cell marker EpCAM by Wnt-beta-catenin signaling in hepatocellular carcinoma. Cancer Res. *67*, 10831–10839.

Zeng, Y.A., and Nusse, R. (2010). Wnt proteins are self-renewal factors for mammary stem cells and promote their long-term expansion in culture. Cell Stem Cell *6*, 568–577.

Zetsche, B., Gootenberg, J.S., Abudayyeh, O.O., Slaymaker, I.M., Makarova, K.S., Essletzbichler, P., Volz, S.E., Joung, J., van der Oost, J., Regev, A., et al. (2015). Cpf1 is a single RNA-guided endonuclease of a class 2 CRISPR-Cas system. Cell *163*, 759–771.